Optoelectronic Master Chip for Optical Computing

Robert J. Lang, Jae H. Kim* , Anders Larsson, Akbar Nouhi, and Jeff Cody
Center for Space Microelectronic Technology
Jet Propulsion Laboratory
California Institute of Technology
Pasadena, California, 91109

Steven Lin and Demitri Psaltis
California Institute of Technology
Pasadena, California, 91109

Richard C. Tiberio, George Porkolab, and E. D. Wolf
National Nanofabrication Facility
Cornell University
Ithaca, New York 14853

Abstract

GaAs optoelectronic integrated circuits (OEICs) require the combination of several types of devices that place widely differing demands upon the layer structure and processing technologies. We report on the development of MESFETs, bipolar transistors, detectors, and a unique class of beam-steered facetless grating surface-emitting lasers and the integration of up to 300 devices of multiple types.

1. Introduction

GaAs-based optoelectronic integrated circuits (OEICs) offer tremendous potential for high-speed communications and computing. Applications for OEICs include as interfaces between conventional electronics, in which the high speed, low loss, and low crosstalk of optical connections are exploited, and computations that make direct use of the properties of light and optoelectronic components, e.g., optical neural networks. Nearly all OEICs incorporate three basic functional elements: detectors, for transforming light into electronic signals, electronics, for processing of electronic signals, and emitters (lasers and/or LEDs) for rebroadcast of the optical signal. A set of integrable devices providing these functions can form a "master chip" that can realize many different functions.

However, the different components of the master chip place conflicting demands upon the optoelectronic technology used in their realization. Lasers and LEDs, for example, are bipolar devices, while MESFETs are unipolar. In addition, the device structures for more sophisticated discrete devices are demanding in themselves, and do not permit significant compromise to accomdate other devices' structures.

In this paper, we report on the technology developed toward construction of such a master chip. All of the devices being pursued are integrable, and several examples of integration are presented.

2. Electronics

Bipolar Devices

Bipolar transistor technology is desirable for optoelectronic integration because the light sources—LEDs and lasers—are typically low-impedance devices that require a current source driver, a role for which

*Currently with Boeing High Technology Center, Seattle, Washington

 0-8194-0691-0/91/$4.00

bipolar transistors are well suited. In addition, double-heterostructure bipolar transistors (DHBTs) offer high gain and high speed operation as well.

However, bipolar transistors are a demanding class of device. An integrable DHBT structure is shown in figure 1 that can supply moderately high beta (~150). The layer structure consists of:

0.1 μm n^+ AlGaAs/GaAs SL buffer
1.2 μm n-$Al_{0.3}Ga_{0.7}As$ collector
0.1 μm u-GaAs spacer
0.3 μm p-GaAs base
0.1 μm u-GaAs spacer
1.0 μm n-$Al_{0.3}Ga_{0.7}As$ emitter
0.23 μm n^+-GaAs cap

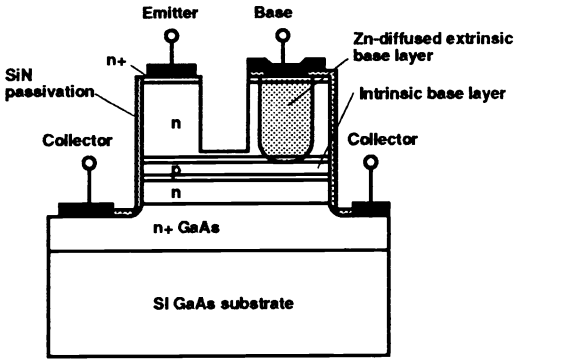

Figure 1. Schematic of the DHBT structure.

The 2 GaAs spacer layers were provided to reduce interdiffusion between the n and p-type layers and the resulting movement of the p-n junction. Contact was made to the base via a Zn diffusion through the emitter layer. It was found to be critical to etch a well between the emitter and the base to prevent recombination across the high-bandgap base-emitter p-n junction. For etching to within 0.1 μm of the base layer, betas typically in excess of 150 were recorded.

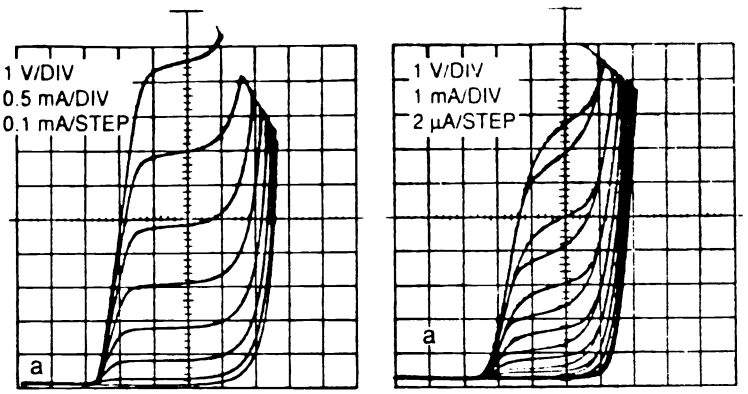

Figure 2. Darlington transfer function of the integration DHBT pairs.

This transistor structure may also be used as a phototransistor by illuminating the base through the high-bandgap emitter. Operation of transistor pairs as photoDarlingtons is shown in figure 2. The same layer structure may also provide an emitter. A diffused DH LED was fabricated along with the photodetector and Darlington-coupled transistor to provide all three functions—light detection, amplification, and emission—from a single structure.

These devices were used to fabricate arrays of optoelectronic neurons. A chip of 300 discrete devices was fabricated; a 10×10 array is shown in figure 3. The individual neurons provided a threshold for firing, set by the bias on the phototransistor, and loop gains via the Darlington pairs of as high as 6000, more than offsetting the relatively low efficiency (~1%) of the LED.

MESFETs

The major disadvantage of bipolar circuitry is a higher quiescent power dissipation; this disadvantage is particularly pronounced in large arrays of devices. To reduce the power dissipation, GaAs MESFETs were integrated with the bipolar LEDs and phototransistors. This required a more complex layer structure, illustrated in figure 4. Three additional layers for the contact and channel of n-channel MESFETs were added below the bipolar layers. The bipolar layers were selectively removed to expose the FET layers, and

a recessed gate was etched into the structure. The remainder of the process was similar to that for the all-bipolar structure. The transfer function, as a function of gate bias, is illustrated in figure 5.

3. Lasers

Lasers in OEICs

Surface-emitting lasers are preferable to LEDs for OEIC emitters due to their higher efficiency, higher modulation speeds, and superior spatial modal properties. Several classes of surface-emitting lasers have been pursued; they are, in increasing difficulty of fabrication, etched-mirror deflector lasers, grating surface emitters, and vertical-cavity lasers. While the last have demonstrated the lowest thresholds and have seen significant progress in recent months, their demanding growth conditions make integration with other devices difficult, while etched-mirror and grating surface emitters, being based on more conventional laser structures, place fewer compromising demands on the electronic devices with which they are integrated.

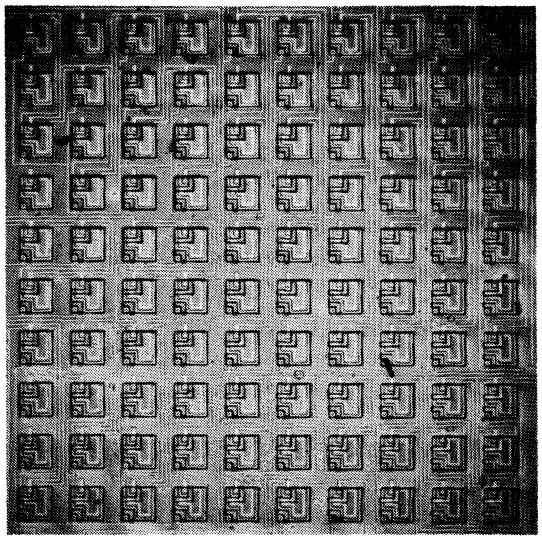

Figure 3. Photograph of the 10×10 array of neurons.

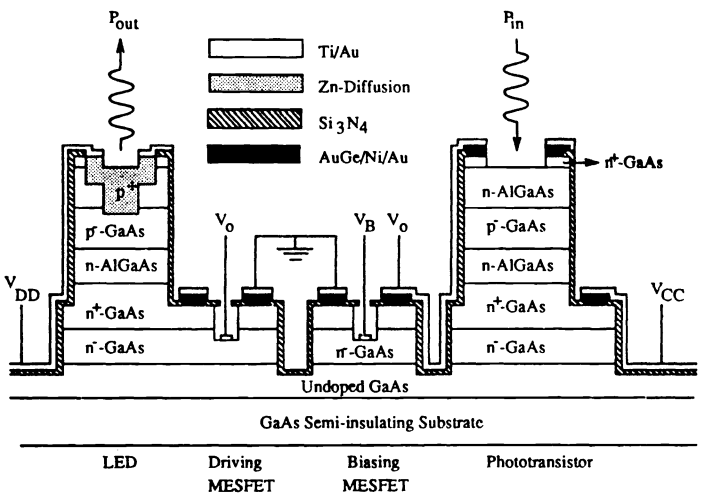

Figure 4. Schematic of the MESFET/bipolar neuron structure.

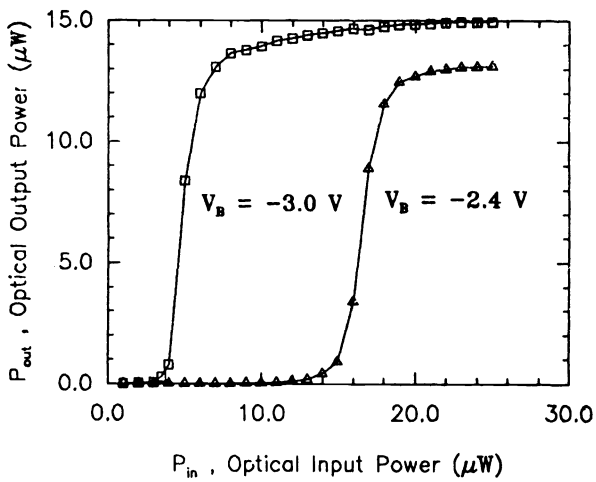

Figure 5. Transfer function of the MESFET/bipolar neuron.

Grating surface-emitting lasers

Grating lasers also offer the potential for very low threshold operation while using a less demanding layer structure. In addition, they offer the unique property that by fabricating more complex grating structures, one may control the shape of the beam to a great degree, achieving, for example, steered and/or focused output beams. For these reasons, single-element grating surface-emitting lasers offer great potential as sources for optical interconnects and large-scale optoelectronic integrated circuits. The full exploitation of

their potential, however, requires fabrication of multiple grating periods and shapes to optimally provide the functions of feedback, output coupling, and beam shaping to the laser.

In this section, we report the fabrication and characterization of hybrid grating lasers incorporating both first- and second-order grating structures to separately provide feedback and output coupling. We will show that a hybrid structure, combining a second-order grating mirror with a first-order grating mirror simultaneously improves the threshold current, quantum efficiency, and vertical far field pattern of the device. In addition, by combining first-order and nonresonant gratings, integration of lasers with beams emitted at multiple angles have been achieved.

The devices were fabricated on a molecular-beam-epitaxy-grown structure. The layer structure consisted of (from the substrate up):

0.1 μm n^+ AlGaAs/GaAs superlattice buffer
1.0 μm n-$Al_{0.6}Ga_{0.4}As$ lower cladding (Si doped: 3×10^{17} cm^{-3})
0.3 μm n-$Al_{0.6-0.2}Ga_{0.4-0.8}As$ GRIN layer (Si doped: 3×10^{17} cm^{-3})
100 Å GaAs active layer
0.3 μm p-$Al_{0.2-0.6}Ga_{0.8-0.4}As$ GRIN layer (Si doped: 3×10^{17} cm^{-3})
1.0 μm p-$Al_{0.6}Ga_{0.4}As$ upper cladding (Si doped: 3×10^{17} cm^{-3})
0.2 μm p^+-$Al_{0.6}Ga_{0.4}As$ contact layer (Si doped: 3×10^{17} cm^{-3})

On this structure, mesas 250 μm wide separated by 250 μm wells were etched using 1:8:8 (H_2SO_4:H_2O_2:H_2O) to expose the GRIN layer. 50 μm×250 μm Cr:Au contacts were evaporated onto the mesa and AuGe/Au contacts evaporated onto the substrate; this permitted a piece to be cleaved off and characterized before the gratings were formed to match the grating period precisely to the wavelength and refractive index of the substrate.

On the remaining piece, 1000 Å of PMMA resist was spun on. 80×80 μm gratings with periods of 122.5 and 245 nm were patterned in the well regions by e-beam lithography, using a JEOL 5DII system; the resist was developed in MIBK and etched by chemically-assisted ion beam etching (CAIBE) in Cl_2. By fabricating the contacts before the the grating, the structure could be tested immediately following the grating fabrication step. The finished device is illustrated schematically and in a photograph in figure 6. By using electron-beam lithography, it was possible to make several devices on the same wafer, permitting direct comparison of convention second-order and hybrid devices.

The devices were tested unmounted under short-pulse conditions (500 ns at 1 kHz repetition rate). Note that no cleaving was required. Light-current curves and quantum efficiencies are illustrated in figure 7. We fabricated two types of device: a conventional device had a second-order grating at each end, while the new hybrid structure had a first-order grating at one end and a second-order grating at the other.

The threshold currents for the hybrid structure are roughly 2/3 those of the conventional structure, due to the higher feedback of the first-order grating. The quantum efficiency is also slightly higher for the hybrid structure, which we also attribute to the increased reflectivity of the first-order grating.

Significant improvement appears in the vertical far field, which is measured along the laser axis for both conventional and hybrid structures. Both show narrow beams with a width comparable to the diffraction limit of the 80 μm emission areas; however, since the conventional all-second-order structure has two such emitting areas, there is a Young's double-slit interference pattern superimposed on the field. The hybrid structure, by contrast, has an extremely smooth far field pattern, due to its single emission region.

In the devices incorporating nonresonant gratings, the first-order grating provided feedback only, with no output coupling; the nonresonant grating provided purely output coupling. As can be seen in the photograph in figure 8, no surface-normal light was emitted from either grating (the bright region around the probe is spontaneous emission). However, as was the design, by measuring the far field at 45° to the substrate, a sharply-defined single lobe was produced, with a far field divergence that was diffraction-limited.

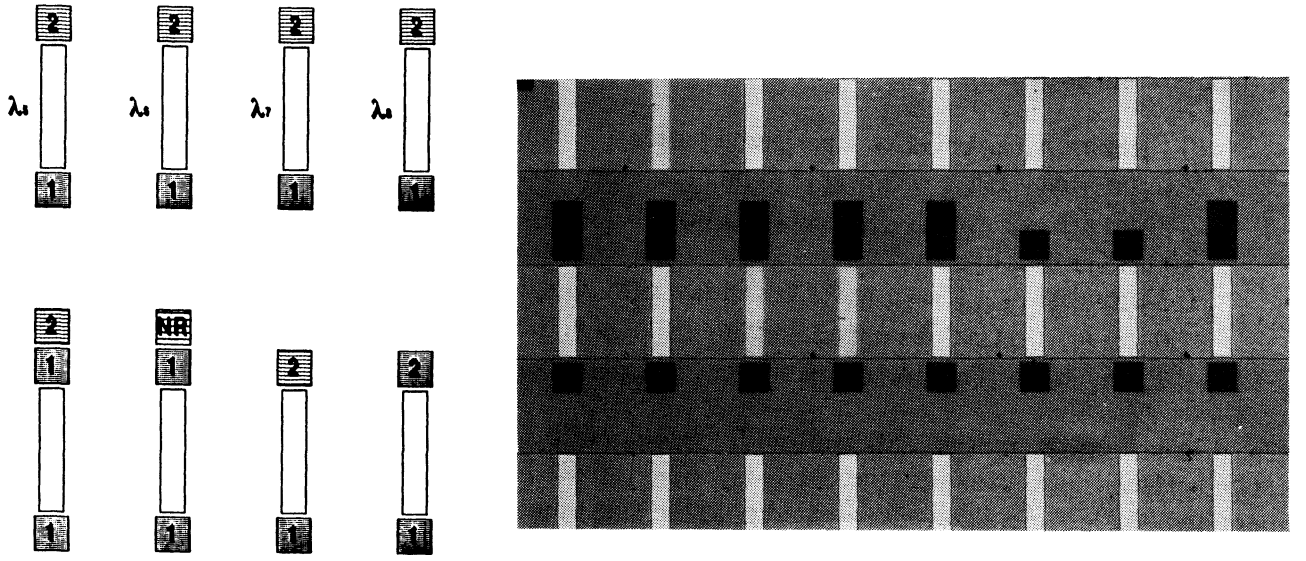

Figure 6. Photograph and schematic of e-beam written grating surface-emitting lasers. 1=first-order grating, 2=second order grating, NR=nonresonant grating.

The quantum efficiency of this first device was quite low. Some part of the degradation can be attributed to scattering loss at the mesa/well interface which we have seen in more conventional devices; this can be eliminated by a more optimized layer structure/grating depth combination that is the subject of current development. The major contribution, however, comes from the low transmission of the first-order grating due to its high reflectivity; by comparing the quantum efficiency of hybrid 1/2 lasers, 1/1-2 lasers and 1/1-NR lasers, we estimate that no more than 10% of the light is transmitted by the first-order grating. This problem is easily solvable by simply reducing the length or depth (and therefore, coupling) of the first-order mirror.

These single-element hybrid first- and nonresonant-order grating surface-emitting lasers have demonstrated narrow, diffraction-limited far fields emitted at large, controllable angles to the substrate. By tailoring the grating period, or integrating multiple gratings into a single device, lasers become possible with multiple-output angle-beams at specified angles. This capability will allow new architectures for direct optical interconnects and optical computers. We further note that by using current injection or temperature tuning, some additional degree of dynamic beamsteering may also be possible. All of the laser structures were fabricated on a conventional single or double quantum well double heterostructure. They therefore offer no greater challenge to integration with electronics than conventional edge-emitting lasers.

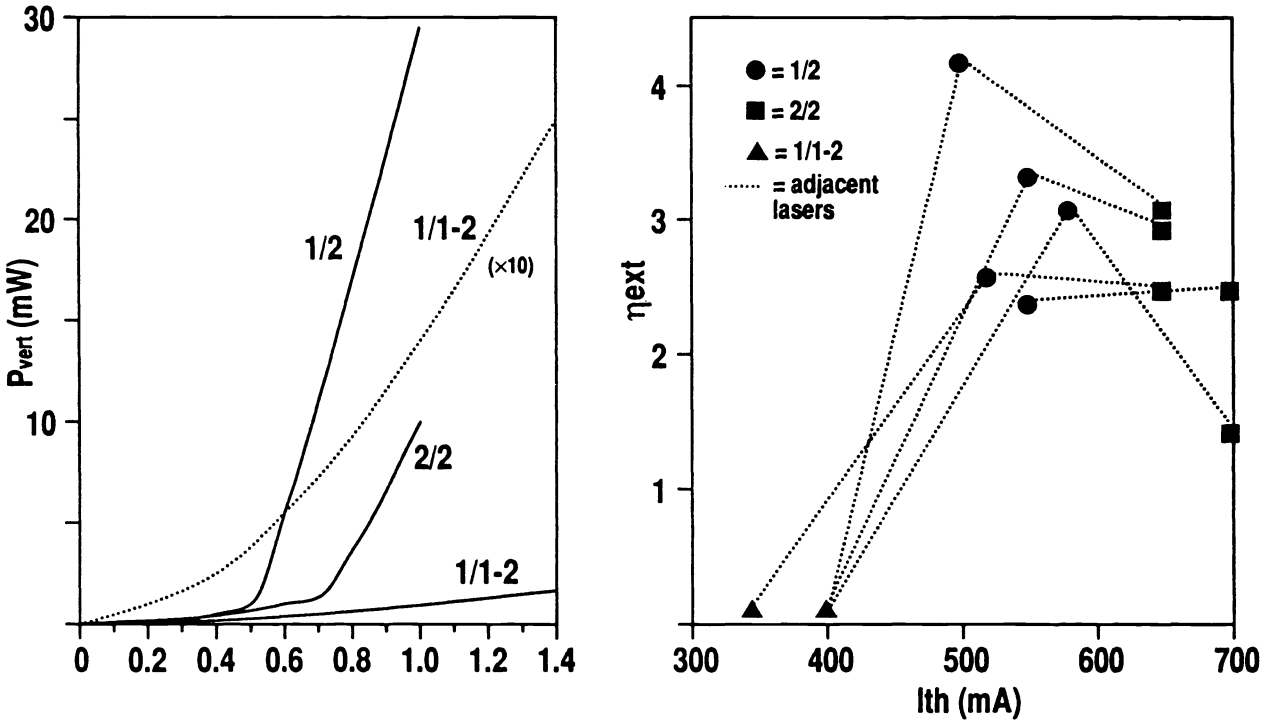

Figure 7. Light-current curves (left) and quantum efficiencies (right) for mixed-grating surface-emitting lasers.

In conclusion, we have demonstrated the development of FET circuitry, bipolar transistor drivers and detectors, LEDs and lasers; we have integrated detectors, emitters, and electronics, and demonstrated a novel class of surface-emitting laser suitable for optoelectronic interconnects and other OEIC circuits.

4. Acknowledgements

The research described in this paper was performed by the Center for Space Microelectronics Technology, Jet Propulsion Laboratory, California Institute of Technology, and was sponsored by the Defense Advanced Research Projects Agency and the Strategic Defense Initiative Organization/Innovative Science and Technology Office through an agreement with the National Aeronautics and Space Administration (NASA). Portions of the research was carried out in collaboration with the California Institute of Technology and the National Nanofabrication Facility, Cornell University.